

## STACKING FAULTS IN KAOLIN-GROUP MINERALS IN THE LIGHT OF REAL STRUCTURAL FEATURES

A. S. BOOKIN,<sup>1</sup> V. A. DRITS,<sup>1</sup> A. PLANÇON,<sup>2</sup> AND C. TCHOUBAR<sup>3</sup>

<sup>1</sup> Geological Institute, Academy of Sciences of the U.S.S.R., Pyzevsky 7, Moscow 109017, U.S.S.R.

<sup>2</sup> Centre de Recherche sur les Solides à Organisation Cristalline Imparfaite and Université d'Orléans, 45100 Orléans, France

<sup>3</sup> Université d'Orléans, Laboratoire de Cristallographie, ERA#841, 45100 Orléans, France

**Abstract**—A comparison of the structural characteristics of the kaolin-group minerals, mainly kaolinite and dickite, shows that they differ in both the two-dimensional periodicity in the 1:1 layers and the rotation angles of the polyhedra. Distortions in a real 1:1 layer, compared with an idealized layer, do not allow such stacking faults as  $\pm 120^\circ$  layer rotations and vacancy displacements, because the second layer is incommensurable with the first. The 1:1 layer structure and the fact that the unit cell is symmetrical with respect to the plane passing through the long diagonal of the unit cell suggest the possibility of defects resulting from the two stacking sequences for the same layers. For a regular alternation of translations, a halloysite-like structure should be the end-member of such a series of defect kaolinite types.

The formation of layers having vacant octahedral C-sites is another possible type of fault. Because of the minor difference between  $\gamma$  and  $90^\circ$ , dickite-like layers should exist. A regular alternation of B and C layers yields dickite as the end-member structure. In materials containing few defects, stacking faults of both types lead to similar X-ray powder diffraction patterns. Thus, the nature of the stacking faults is difficult to determine experimentally. In materials containing many defects, however, the two models lead to different calculated diffraction patterns. Therefore, only a study of defect-rich types of kaolinite can determine which types of defects exist in natural kaolinite samples.

**Key Words**—Defect structures, Dickite, Kaolinite, Stacking faults, X-ray powder diffraction.

**Резюме**—Сравнение структурных характеристик минералов каолиновой группы, в основном каолинита и диккита, показало, что они различаются как в отношении двумерной периодичности их 1:1 слоев, так и углами разворота полиэдров. Исхождения реальных 1:1 слоев по сравнению с идеализированными не позволяют реализоваться таким дефектам упаковки, как вращения на  $\pm 120^\circ$  и смена положения вакансии, поскольку второй слой оказался бы несоизмеримым с первым. Строение 1:1 слоя и элементарной ячейки, будучи симметричны относительно плоскости, проходящей через длинную диагональ элементарной ячейки, предопределяют возможность возникновения дефектов упаковки, вызванных двумя способами наложения одготипных смежных слоев. В случае их регулярного чередования конечным членом такого ряда дефектных каолинитов была бы структура галлузитового типа.

Возникновение слоев с вакантной С позицией представляется другим допустимым типом ошибок. Вследствие малого отклонения угла гамма от  $90^\circ$  могли бы встречаться диккито-подобные встройки, давая при упорядоченном чередовании слоев В и С диккит как конечный член ряда. В образцах с низким содержанием дефектов оба типа ошибок приводят к близкому профилю рентгеновской дифракции и природу ошибок экспериментально установить сложно. В образцах с высокой концентрацией дефектов две модели ведут к различным дифракционным картинкам, поэтому изучение сильно дефектных каолинитов может ответить на вопрос, какой тип дефектов встречается в природный образцах.

### INTRODUCTION

The theory of phyllosilicate polytypism yields a systematic derivation of all the members of a given polytype group. For example, 6 one-layer and 22 two-layer polytypes have been predicted for the kaolin-group minerals (Newnham, 1961; Zvyagin, 1964). Based on these results, Zvyagin (1964) predicted the structure of nacrite. Polytypism theory is generally based on idealized structures. This is a serious limitation when trying to choose the most stable structure, or when predicting the direction of polytype transformations. For example, the theory hardly explains why only three kaolin-

group minerals (kaolinite, dickite, and nacrite) occur in nature, with kaolinite being by far the most abundant. In addition, the status of halloysite among the theoretically derived polytypes remains unclear. Newnham (1961) showed that accurate descriptions of real structural details must be used to understand the relative stabilities and abundances of different kaolin-group minerals.

If studied by various physico-chemical methods, the kaolin-group minerals, especially kaolinite itself, display an extreme diversity. X-ray powder diffraction patterns of different kaolinite samples differ in the

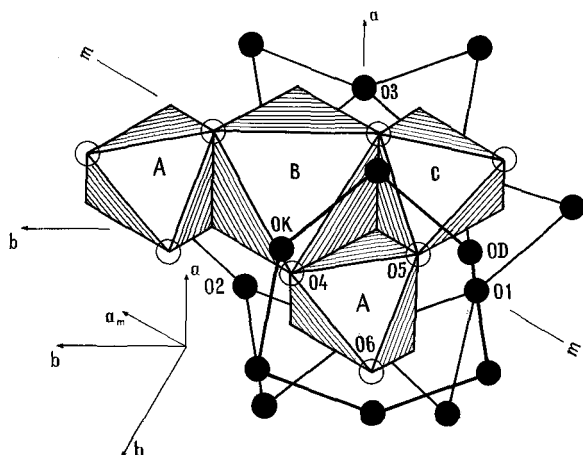


Figure 1. Dioctahedral 1:1 layer with B site vacant. Open circles = inner-surface hydroxyls; solid circles = basal oxygens; the thick line shows the hexagonal ring of the neighboring tetrahedral sheet; OK-OI in kaolinite; OD-OI in dickite; A, B, and C denote octahedral sites as proposed by Bailey (1980).

amount of broadening of various reflections. These differences are the direct result of the presence of layer stacking faults. Several attempts have been made to understand the nature of the stacking faults in kaolinite (Brindley and Robinson, 1946; Mitra and Bhattacharjee, 1970; Murray, 1954; Plançon and Tchoubar, 1977a, 1977b; Tchoubar *et al.*, 1982). These workers based their concepts on an idealization of the kaolinite structure.

Heretofore, the proposed models of the defect structure have lacked a firm crystal chemical foundation. The basis of the present work is that the nature of the stacking faults in a phyllosilicate is largely determined by the specific structural features of the material in question. The objective of the present paper is to present a new view of the stacking faults in kaolinite that is in harmony with the known structural and crystal chemical features of this mineral.

#### STRUCTURE OF 1:1 LAYERS AND STACKING SEQUENCES IN KAOLIN-GROUP MINERALS

The basic structural element in all kaolin-group polytypes is a 1:1 layer consisting of a tetrahedral sheet and an octahedral sheet linked together by a common plane of oxygens and hydroxyls. Of the octahedral sites,  $\frac{2}{3}$  are occupied by Al. Bailey (1980) labeled the three non-equivalent sites A, B, and C (Figure 1); for the purposes of this paper, a 1:1 layer will be denoted by a letter corresponding to a vacant octahedral site. Ideally, an isolated 1:1 layer can be described in terms of a C-centered unit cell having  $b/a = \sqrt{3}$ . Adjacent layers are stacked so that one of the inner-surface hydroxyls and a basal oxygen of the adjacent layer are paired, favoring the formation of long hydrogen bonds.

Table 1. Rotation angles of polyhedra in kaolin-group minerals.

Mineral	Tetra- hedral rotation	Octa- hedral (O,OH) base rotation	Octa- hedral O base rotation	Reference
Dickite	6.7°	8.3°	8.0°	Joswig and Drits (1986)
Nacrite	7.3	7.1	5.4	Blount <i>et al.</i> (1969)
Kaolinite	11.5	5.0	3.0	Zvyagin (1960)
Kaolinite	10.5	6.5	4.0	Drits and Kashaev (1960)
Kaolinite	7 (1)	6 (1)	8 (1)	Suitch and Young (1983)

Successive B layers in an idealized kaolinite are shifted by  $-a/3$  with respect to one another. This yields a one-layer monoclinic cell. In idealized dickite, successive layers are rotated by  $\pm 120^\circ$ , so that for fixed  $\vec{a}$  and  $\vec{b}$ , the vacancy alternates between B and C sites, and a two-layer unit cell is formed. Figure 1 shows the pairing of basal oxygens and hydroxyls for kaolinite and dickite interlayers. The two-layer periodicity in nacrite results from a rotation of adjacent layers by  $\pm 60^\circ$ .

The kaolin-group polytypes were derived under the assumption that each of them consists of identical layers. This seems true for the chemical composition, inasmuch as all natural kaolin-group minerals have practically no ionic substitutions. The refined structural data presently available can be used to determine whether the 1:1 layers in the different kaolin-group minerals are indeed structurally identical.

#### Dickite and nacrite

The structure of dickite has been refined to the highest precision (Rozdestvenskaya *et al.*, 1982; Sen Gupta *et al.*, 1984; Joswig and Drits, 1986) compared with the other polytypes. Even the preliminary refinement of Newnham (1961) revealed substantial deviations in the real layer structure from the idealized model. For example, the counter rotation of octahedral basal oxygens leads to an increase in the dimensions of the vacant octahedron, whereas tetrahedral rotation transforms the hexagonal hole in the tetrahedral sheet into a ditrigonal hole (Figure 1). Similar structural distortions were found for the nacrite 1:1 layer (Blount *et al.*, 1969). Tetrahedral and octahedral rotation angles for the structures in question are given in Table 1.

If it is considered as an isolated unit, a layer is deprived of all symmetry elements except translation. Although cations in a layer seem to be related by a mirror plane  $m$  (Figure 1), a mirror plane is not a true symmetry element in space group  $Cc$ . The basal surface of tetrahedra is corrugated in both dickite and nacrite because of displacements of the basal oxygen O1 which lies in the  $m$  plane. In the most accurate dickite structure refinements, deviations of the hydroxyl surface

Table 2. Atomic coordinates of a separate 1:1 dickite layer in the  $\{a_m, b_m, c^*\}$  unit cell.

Atom	X/a	Y/b	Z (Å)
O1	-0.268	0.267	0.002
O2	-0.268	-0.265	-0.002
O3	-0.464	0.001	0.190
O4	-0.005	0.309	2.266
O5	-0.004	-0.309	2.262
O6	0.074	0.000	2.336
O7	-0.116	0.193	4.322
O8	-0.118	-0.192	4.356
O9	0.309	0.001	4.318
Si1	-0.003	0.329	0.672
Si2	-0.003	-0.329	0.664
Al1	-0.307	0.335	3.407
Al2	-0.307	-0.335	3.396

from planarity became especially clear, resulting from the displacement of one of the independent OH groups (O5 in Figure 1) outside the octahedral sheet. The other two inner-surface hydroxyls are at the same level, at least within experimental error. Oxygen O1 and hydroxyl O5 form one of the hydrogen bond pairs. The displacement of the OH is by a factor of 10 less than that of O, so that the latter cannot compensate completely for the increase in the H-bond distance. Nevertheless, the observation that the cavities and protuberances of the dickite layer are paired in adjacent layers was interpreted by Newnham (1961) as favoring the formation of dickite in nature, because this arrangement shortens the interlayer hydrogen bond.

Possibly, the OH displacement may not be an inherent property of a 1:1 layer, but a reaction to the stretching of the O—OH bond resulting from the depression of the basal oxygen. This assumption is supported by a similar matching of interlayer surfaces in nacrite, although the corrugation results from the shift of a different atom.

The dickite structure contains a peculiar feature that has not been mentioned in the literature. To demonstrate this, the experimental atomic coordinates (Joswig and Drits, 1986) were transformed to a new unit cell. The origin was taken at the center of a hexagonal ring, axes  $a_m$  and  $b_m$  were chosen as in Figure 1, and  $c^*$  was directed from tetrahedron to octahedron. To a high degree of accuracy, the atomic positions for this unit cell can be seen to be related by a mirror plane passing through the origin and parallel to  $m$  (Table 2). Thus, the pseudo-symmetry plane  $m$ , mentioned above, indeed reflects the layer symmetry, although the space group does not require it.

### Kaolinite

The structure of kaolinite is known with less precision, although several attempts have been made to refine its structure by various diffraction methods. The main difficulty is associated with the small particle size

and the defect structure of this mineral. The only single crystal refinement available in the literature lacked sufficient accuracy, because only intensities for the  $h0l$  and  $0kl$  reflections were measured photographically (Drits and Kashaev, 1960). This refinement was criticized by Bailey (1980) because of supposed twinning of the crystal, but, in fact, the crystal was not twinned, but was bent in an umbrella-like shape. A refinement based on oblique-texture electron diffraction patterns recorded on photographic film was also insufficiently precise (Zvyagin, 1960).

Both X-ray and neutron powder diffraction have been used more recently for the refinement of 1:1 phyllosilicate structures (Adams and Hewat, 1981; Suitch and Young, 1983; Thompson and Cuff, 1985). The poor agreement between the dickite structure refinement by the Rietveld powder method (Suitch and Young, 1983) and single crystal refinements suggests that the data presented by Suitch and Young (1983) are not sufficiently accurate to allow a discussion of structural details. One of the important sources of errors in the Rietveld refinement of Suitch and Young (1983) may have been the preferential orientation of the sample, which was not taken into account in the refinement. Obviously, the greater the angle between the diffracting and cleavage planes, the greater the experimental error in the intensity, so that the smallest error is expected for the  $00l$  reflections. The smaller errors for the  $00l$  reflections might explain the relatively higher accuracy in the determination of  $z$ -coordinates in that study. In addition, Suitch and Young (1983) rejected the centering of the unit cell in the kaolinite structure. To reduce the considerable scatter in the atomic coordinates obtained by different authors, the data of Suitch and Young (1983) have been converted to the average C-centered unit cell.

From the foregoing discussion, none of the kaolinite refinements available is clearly more reliable than any other.

### Distortions of coordination polyhedra

Until recently, a certain ambiguity has existed concerning the position of the vacant octahedron in the kaolinite layer. Bailey (1980), for example, assumed that both B and C layers were indistinguishable by X-ray powder diffraction; however, all the kaolinite structure refinements mentioned above, if brought to a conventional unit cell having  $\alpha > 90^\circ$  and  $\gamma < 90^\circ$  indicate that it is the B site that is vacant. Bailey's statement is correct for an idealized kaolinite polytype having  $\alpha = \gamma = 90^\circ$ . In the real unit cell, replacement of C layers by B layers leads to a substantial intensity redistribution (Figure 2). The mathematical formalism used to calculate the X-ray diffraction patterns for crystals having different types of structural defects as well as for structures not having defects was described by Plançon and Tchoubar (1977b), Plançon (1981), and

Sakharov *et al.* (1982). Thus, in terms of the conventional unit cell, regular kaolinite consists only of B layers and never of C layers.

Octahedral and tetrahedral rotation angles in kaolinite, as reported by different workers, are given in Table 1. According to Suitch and Young (1983), the kaolinite 1:1 layer is similar to that of dickite, whereas Zvyagin (1960) and Drits and Kashaev (1960) found greater tetrahedral rotation and a smaller rotation of the hydroxyl bases of the octahedra than in dickite.

#### Interlayer structure

In 1:1 phyllosilicates, rotation of polyhedral bases leads to changes in the O–OH distances across the interlayer region. The distances increase with increasing rotation of the OH-bases and decrease with increasing tetrahedral rotation (Figure 1). Thus, the structures proposed by Zvyagin (1960) and Drits and Kashaev (1960) imply a shorter hydrogen bond length than the dickite-like structure, other parameters being equal.

According to Zvyagin (1960), the corrugation of the tetrahedral basal plane in kaolinite is unusual in that one of the three non-equivalent basal oxygens is shifted outside the tetrahedral sheet. Suitch and Young (1983), however, who used more reflections to refine the structure of the well-crystallized Keokuk kaolinite, found that the corrugation pattern is similar to that in dickite, nacrite, and other dioctahedral phyllosilicates. The less distinct deviations of the hydroxyl surface from planarity was probably beyond the experimental precision.

Assuming that the layers are identical for the different polytypes, Newnham (1961) inferred that in kaolinite the cavities in the basal oxygen network would not match the protuberances in the hydroxyl sheet. This mismatch would weaken one of the hydrogen bonds, and for this reason kaolinite should be less stable than dickite or nacrite. This interpretation, however, is doubtful in the light of the structural data now available. Using a more realistic pattern of basal oxygen corrugation and assuming that OH displacements result from an attempt to shorten hydrogen bonds, the buckling of the kaolinite hydroxyl surface is probably determined by hydroxyl O4 (Figure 1). This distortion was proposed by Zvyagin (1960), although the accuracy in coordinates was lower than the displacement itself. Thus, all kaolin-group polytypes appear to be equivalent in terms of the matching of adjacent corrugated surfaces.

### UNIT CELLS OF THE KAOLIN-GROUP MINERALS

In contrast to the remarkable reproducibility of different dickite structure refinements, the deviations in the unit-cell parameters of this mineral are much greater than the estimated errors (Table 3). Note that the two determinations listed in Table 3 that differ most (Joswig and Drits (1986) and Rozdestvenskaya *et al.*

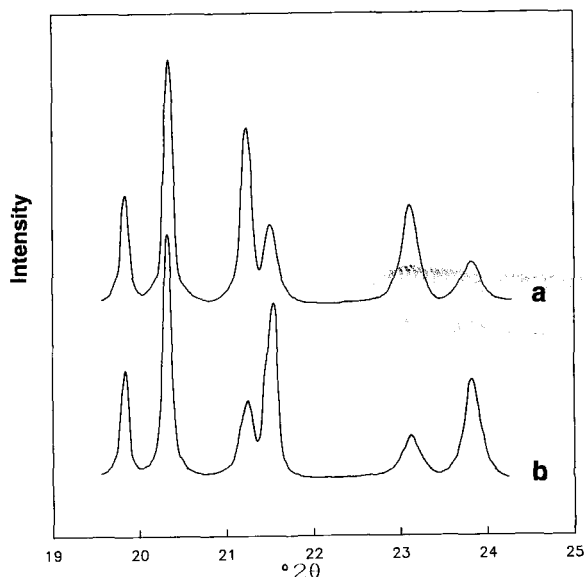


Figure 2. Simulated X-ray powder diffraction profiles for regular kaolinites having vacant B (a) and C (b) sites in the region of the 02,11 reflections.

(1982)) were carried out on crystals from the same sample, but in different laboratories using different X-ray wavelengths. The disparity between these two determinations implies the existence of systematic errors rather than real variations in the parameters of crystals of different origins. The existence of systematic errors is confirmed by the ratio  $b/a$  given in Table 3. The difference between the maximum and the minimum estimated  $a$  and  $b$  is about 0.25%, whereas that for  $b/a$  is only 0.05%.

#### Dickite unit cell

To eliminate as much error as possible, all the linear parameters in Table 3 were normalized to the  $b$  value of Suitch and Young (1983). The corrected values given in parentheses in Table 3 reproduce both the parameter  $a = 5.148 \text{ \AA}$  and the interlayer distance  $d(001) = 7.161 \text{ \AA}$ , with an error of about  $0.001 \text{ \AA}$ . The only exception is the  $a$  parameter reported by Sen Gupta *et al.* (1984), which corresponds to the ideal unit-cell ratio  $b/a = \sqrt{3}$ . Most refinements indicate that the dickite 1:1 layer unit cell is elongated with respect to this ideal ratio.

The interlayer-shift component parallel to  $\vec{a}$ ,  $t_a = c \cos \beta/2$ , is close to  $a/3$  (Table 3). If the origin of a layer is chosen at a point invariant to rotations of the layer and vacancy displacements, e.g., at the center of the hexagonal ring, the interlayer shift along  $b$ ,  $t_b$ , can also be found. This component, which should be zero in the idealized structure, is actually well reproduced in the different refinements and equals  $0.024 b$ . Because the shifts are of opposite signs for two adjacent pairs of layers, the two-layer dickite unit cell is monoclinic.



## Kaolinite unit cell

Table 3 illustrates the differences in the conception of the kaolinite unit cell. An idealized 1:1 layer having  $b = a\sqrt{3}$  and  $\gamma = 90^\circ$  is replaced by that having  $\gamma < 90^\circ$  and  $b/a > \sqrt{3}$ . Differences in estimated cell dimensions may have resulted from systematic errors, as well as from shifts of reflections resulting from stacking faults. For kaolinite, observed cell dimensions might really depend on the genesis of the sample, the amount of defects, or other factors.

The data of Suitch and Young (1983) seem the most reliable, due to the structural perfection of the Keokuk kaolinite, as well as to the good reproducibility of results for two different samples. To make the cells of kaolinite and dickite comparable, the data in Table 3 were normalized to the  $b$  parameter of their study. According to Suitch and Young (1983) both  $a$  and  $b$  for the Keokuk kaolinite are greater than the comparable values for dickite, although the  $b/a$  ratios are similar (cf. Table 3). The increase in the kaolinite cell confirms indirectly the smaller octahedral rotation compared with that of dickite (Table 1), because, for constant edge length,  $b$  decreases with an increase of octahedral rotation. On the contrary, the layer shift along  $c^*$  in kaolinite is 0.01 Å less than in dickite. As a result, the volumes of the cells in terms of one layer differ by less than 0.03%.

The 1:1 layer thickness, measured as the difference between the  $z$ -coordinates of the hydroxyl sheet and the basal oxygens (regardless of the corrugation), in dickite and nacrite are 4.32 and 4.31 Å, respectively. For kaolinite, different authors report layer thicknesses ranging from 4.29 to 4.43 Å. If the layer thickness is assumed to be constant for all the minerals in question, the repeat distance along  $c^*$  in kaolinite results from a decrease in the interlayer separation. This decrease in interlayer separation also favors shortening of the hydrogen bonds in kaolinite. The in-plane components of the translation vector  $t_a$  and  $t_b$  calculated from the unit cell of the Keokuk kaolinite are  $\{-0.369 \vec{a}, -0.024 \vec{b}\}$ . If the structures of kaolinite and dickite are analyzed in terms of the same coordinate system, i.e., the initial layer in dickite is a B layer, their  $t_b$  vector will not only have the same value, but also the same sign. Hence,  $t_b$  does not depend on the vacancy position in the layer, but it is affected only by peculiarities of the asymmetric hydroxyl network of the preceding layer.

The  $t_a$  vector in kaolinite differs substantially from that for dickite. It follows from Figure 1 that a minor change in  $t_a$  stretches the O6–O3 bond length, shortens the OK–O4 bond length, and does not affect the O5–OD bond length, so that the mean hydrogen bond length is preserved. Both the increase in  $t_a$  and the sign of  $t_b$  however, shorten the O4–OK bond, which is the longest because of the tetrahedral tilt.

Table 3. Unit-cell parameters of dickite and kaolinite.

		Dickite					Kaolinite							
$a$ (Å)	$b$ (Å)	$c$ (Å)	$\beta$	$d(002)$ (Å)	$(b/a)^2$	$t_c/a$	References	$a$ (Å)	$b$ (Å)	$c$ (Å)	$\beta$	$\gamma$	$d(001)$ (Å)	References
5.150 <sub>1</sub>	(5.149)	8.940 <sub>1</sub>	96.73°	(14.420)	(7.160)	3.013 <sub>2</sub>	Newham (1961)	5.13	8.89	7.25	104.67°	90°	7.01	Zvyagin (1960)
5.150 <sub>3</sub>	(5.147)	8.943 <sub>4</sub>	96.76°	(14.421)	(7.161)	3.015 <sub>4</sub>	Rozdestvenskaya <i>et al.</i> (1982)	5.14	8.93	7.37	104.5°	90°	7.13	Drits and Kashaev (1960)
5.1460 <sub>3</sub>		8.9376 <sub>5</sub>	96.76°			3.016 <sub>1</sub>	Suitch and Young (1983)	5.146	8.946	7.388	104.7°	89.9°	7.143	Brindley (1961)
5.149 <sub>2</sub>	(5.158)	8.922 <sub>2</sub>	96.76°	(14.420)	(7.159)	3.002 <sub>4</sub>	Sen Gupta <i>et al.</i> (1984)	5.155	8.959	7.408	104.87°	89.94°	7.156	Goodyear and Duffin (1961)
5.138 <sub>2</sub>	(5.149)	8.918 <sub>2</sub>	96.74°	(14.421)	(7.161)	3.013 <sub>4</sub>	Joswig and Drits (1986)	5.147	8.947	7.418	104.99°	89.96°	7.162	Noble (1971)
Mean	(5.148)			(14.421)	(7.161)	3.014		5.153	8.941	7.403	104.86°	89.82°	7.152	Suitch and Young (1983)

Values in parentheses = normalized to  $b$  values of Suitch and Young (1983).

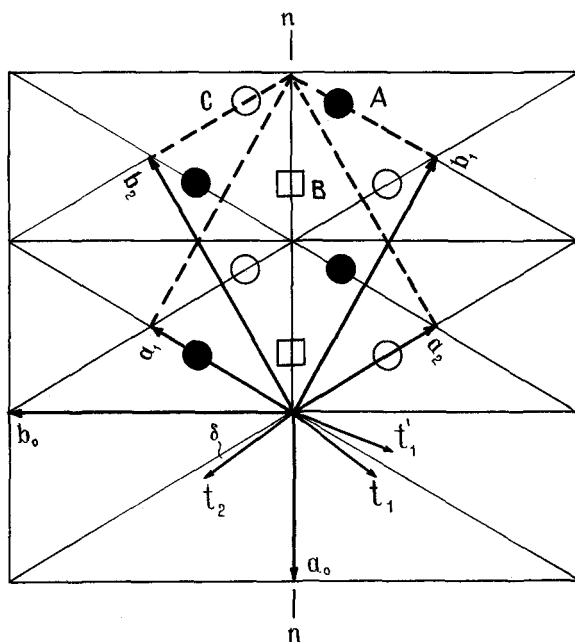


Figure 3. Possible unit cells for a 1:1 layer and octahedral vacancies in kaolinite (squares) and dickite (circles). Detailed comments are given in the text.

#### Comparison of kaolinite and dickite 1:1 layers

The above data suggest that the 1:1 layers in kaolinite and dickite are not identical. Even if the increase in the  $a$  and  $b$  parameters of kaolinite (which might be the result of systematic errors) is real, the kaolinite lattice having  $\gamma < 90^\circ$  cannot be brought into coincidence with the orthogonal lattice of a dickite layer. This statement, however, requires additional analysis inasmuch as three sets of axes can be chosen in a dioctahedral 1:1 layer. These sets of axes are totally equivalent in the idealized case. To elucidate the effect of a lack of hexagonal lattice symmetry in the 1:1 real layers on the possible cell parameters, a layer having the possible coordinate axes marked in Figure 3 should be considered. The unit cells are denoted by  $\{a_1b_1\gamma_1\}$ ,  $\{a_2b_2\gamma_2\}$ , and  $\{a_0b_0\gamma_0\}$ . If the parameters are known for one of the cells, e.g., for  $\{a_1b_1\gamma_1\}$ , those for the other two cells are readily obtained for the C-centered lattice.

$$\begin{aligned} 4a_i^2 &= a_1^2 + b_1^2 \pm 2a_1b_1\cos\gamma_1 \\ 4b_i^2 &= 9a_1^2 + b_1^2 \pm 6a_1b_1\cos\gamma_1 \\ \cos\gamma_i &= (a_i^2 + b_i^2 - 4a_1^2)/2a_1b_1, \end{aligned} \quad (1)$$

where  $i = 0, 2$ .

The superscript in Eq. (1) corresponds to the cell  $\{a_0b_0\gamma_0\}$ . The experimental and calculated parameters for the Keokuk kaolinite are given in Table 4. Note the excellent agreement between  $a_1, b_1, \gamma_1$  and  $a_2, b_2, \gamma_2$ .

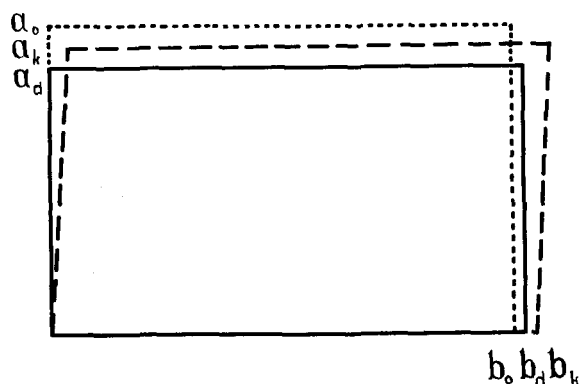


Figure 4. Superposition of dickite unit cell (d) on the conventional (k) and orthogonal (o) kaolinite cells.

Because the acute angle  $\gamma_2$  is obtained exactly for the  $b_2$  direction shown in Figure 3, the  $\{a_1b_1\gamma_1\}$  and  $\{a_2b_2\gamma_2\}$  cells are related by a mirror plane instead of a rotation axis, i.e., they are enantiomorphic. As expected, the  $\{a_0b_0\gamma_0\}$  cell is practically orthogonal. Thus, although the lattice of a layer is not strictly hexagonal even for regular kaolinite, it is not totally asymmetric. To emphasize the presence of a mirror plane in the two-dimensional lattice of a layer, the kaolinite unit cell can be chosen in terms of the axes  $\{a_0b_0\gamma_0\}$ . The unit-cell parameters then are:  $a_0 = 5.167$ ,  $b_0 = 8.917$ ,  $c_0 = 7.403$  Å,  $\alpha_0 = 102^\circ$ ,  $\beta_0 = 98.8^\circ$ , and  $\gamma_0 = 90^\circ$ . Figure 4, drawn out of scale, compares the orthogonal unit cells for kaolinite and dickite layers. For kaolinite,  $a_0$  is greater than  $a_d$  for dickite, whereas  $b_0$  is less than  $b_d$ , leading to  $b_0/a_0 < \sqrt{3}$ .

It is of some interest to examine whether the relationships found for Keokuk kaolinite are valid for the other kaolinites in Table 3. Using Eq. (1), the condition for the equivalence of the two cells is readily obtained:

$$2\cos\gamma = \sqrt{b_1/a_1} - 3\sqrt{a_1/b_1}. \quad (2)$$

For  $b/a = \sqrt{3.020}$  reported by Goodyear and Duffin (1961),  $\gamma_1$  should be  $89.67^\circ$ . Inasmuch as the actual  $\gamma_1$  is greater than this value, condition (2) is not obeyed, the cell  $\{a_2b_2\gamma_2\}$  is not symmetric to  $\{a_1b_1\gamma_1\}$ , and  $\{a_0b_0\gamma_0\}$  is not orthogonal. Condition (2) holds strictly for none of the samples except the Keokuk kaolinite. Only a detailed analysis of each of the kaolinites can indicate whether the violation of condition (2) implies the existence of errors in the determination of the parameters or whether the rule is valid only for well-crystallized kaolinite samples.

The distribution of octahedral cations in 1:1 layers may be visualized by considering Figure 3. In dickite layers one of the sites shown as circles may be vacant. If that vacancy corresponds to an open circle (C site), the origin being at the center of the hexagonal ring, the approximate coordinates for the vacant site in terms

Table 4. Periodicity of a separate 1:1 layer of regular Keokuk kaolinite.

Set of parameters	i = 1	2	0
<i>a</i>	5.153	5.153	5.167
<i>b</i>	8.941	8.941	8.917
$\gamma$	89.82°	89.82°	90.00°
$(b/a)^2$	3.010	3.010	2.978

of the orthogonal axes of dickite are (1/6, 1/6). According to the kaolinite structure refinement, the vacancy (shown as a square in Figure 3) is also at (1/6, 1/6), but in terms of the oblique cell  $\{a_1b_1\gamma_1\}$ . In terms of the orthogonal kaolinite coordinate system  $\{a_0b_0\gamma_0\}$  the vacancy is at  $(-1/3, 0)$ .

Thus, Figures 3 and 4 suggest criteria by which kaolinite and dickite may be distinguished, even on the level of isolated layers: (1)  $b/a > \sqrt{3}$  for dickite and  $b_0/a_0 < \sqrt{3}$  for kaolinite; and (2) in kaolinite the vacancy lies in the plane *n*, whereas in dickite it does not. Therefore, in kaolinite the *n* plane coincides with the mirror plane *m*; in dickite these planes make an angle of 120°. The description of the kaolinite structure in terms of the  $\{a_0b_0\gamma_0\}$  cell is not merely of theoretical interest. Thompson and Cuff (1985) found that the vacant site in the kaolinite: DMSO intercalate is in the *n* plane and  $(b/a)^2 = 2.987$ . Thus, intercalation not only increased the interlayer spacing but also changed the stacking sequence so that adjacent layers were shifted along  $\vec{a}_0$ .

#### PREVIOUS MODELS FOR STACKING FAULTS

X-ray powder diffraction patterns from kaolinites vary in peak positions, resolution, and intensity (see, e.g., Brindley, 1980). Basal reflections 00*l*, however, indicate a fairly large number of parallel, coherently scattering layers. Thus, stacking faults do not violate the periodicity along *c*\*. Reflections of different types were found not to have an identical sensitivity to the presence of stacking faults. Reflections having  $k \neq 3n$  shifted, broadened, or disappeared to a greater degree than those having  $k = 3n$ . Thus, even a qualitative analysis imposes limitations on possible models for stacking faults.

##### The $\pm b/3$ model

The Brindley and Robinson (1946) model, based on  $\pm b/3$  random layer shifts, assumed that the hydroxyl sheet in an idealized layer would coincide with itself after such displacements. To allow for layer structure distortions, Brindley (1980) later proposed that the shifts only approximate  $\pm b/3$  to ensure the proper matching of basal oxygens and hydroxyls. This modification, however, seems also insufficient. As a result of a shift by  $-b/3$ , all the octahedral cations appear exactly above

Si of the adjacent layer. As noted by Newnham (1961) and supported by the electrostatic energy calculations of Giese (1982), this arrangement corresponds to the so-called "monoclinic kaolinite" and is energetically unfavorable, thereby explaining why "monoclinic kaolinite" has not been found in nature. To improve the model, the probabilities for the shifts leading to an unfavorable stacking should therefore be reduced or even set to zero.

##### The $\pm 120^\circ$ model

The model proposed by Murray (1954) was based on the assumption that after a  $\pm 120^\circ$  rotation, a layer coincides with itself, except for the position of the vacant site. Figures 3 and 4 and Table 4 prove that this model is entirely unrealistic. After rotation by  $\pm 120^\circ$  around the center of the hexagonal ring, the basal oxygen of a given ring will indeed occupy nearly the same position, but this is not true for the centers of other rings. After a clockwise rotation,  $\vec{a}_1$  could be brought into coincidence with  $\vec{a}_2$  in both value and direction. The rotation angle is close but not equal to  $120^\circ$ . Directions of  $\vec{b}_1$  and  $\vec{b}_2$ , however, would then differ by  $0.4^\circ$ , so that the center of the hexagonal ring that is separated by  $18 \text{ \AA}$  from the rotation axis ( $2 \times b$ ) would shift by an additional  $0.1 \text{ \AA}$ . To avoid an accumulation of the error, the layer periodicity would have to be violated, leading to very small coherent domain size. Kaolinite coherent domains, however, are known to be as large as hundreds of Ångströms (Plançon and Tchoubar, 1977b; Tchoubar *et al.*, 1982). With a counter-clockwise rotation,  $\vec{a}_1$  can coincide with  $\vec{a}_0$  only in direction, but not in value, whereas  $\vec{b}_1$  and  $\vec{b}_0$  cannot even be made parallel. In other words, the initial 1:1 layer and the rotated one cannot be described in terms of a common lattice.

##### The vacancy displacement model

Plançon and Tchoubar (1977b) proposed a model for the defects in kaolinite that was a compromise between the above two models. The main assumption was that a crystal consists of identically oriented layers, in which vacancies can be located at any of the A, B, or C sites, fixed for each layer. Thus, the difficulty discussed above was overcome. Each layer type is associated with a specific interlayer translation coinciding with or differing by  $\pm b/3$  from the experimental translation in kaolinite. For a block of layers of the same type, the translation is chosen so as to ensure the kaolinite-like stacking sequence.

Proportions for the three layer types and probabilities for transitions from one layer type to another are the parameters of the model. Plançon and Tchoubar (1977b) used a set of parameters leading to a segregation of layer types to form fragments consisting of layers of the same type. A decrease in the probability for stacking faults should lead to an increasing thick-

Table 5. Parameters for conventional unit cells for defectless fragments having different vacancy positions.

Vacancy position Translation	B $\vec{t}_0$	C $\vec{t}_0 + \vec{b}/3$	A $\vec{t}_0 - \vec{b}/3$
<i>a</i>	5.155	5.166	5.170
<i>b</i>	8.959	8.940	8.932
<i>c</i>	7.408	7.389	7.301
$\alpha$	91.68°	87.89°	90.41°
$\beta$	104.87°	104.26°	101.42°
$\gamma$	89.94°	89.90°	89.87°

ness of defect-free fragments. In the limiting case, each sample of kaolinite should consist of a physical mixture of three different crystals. The conventional unit-cell parameters were calculated using translations given by Plançon and Tchoubar (1977b) and are presented in Table 5. Thus, the model predicts an equal abundance for the three kaolinite types, whereas samples having only the first unit cell are found in nature. A fragment consisting of A layers with a translation of  $\vec{t} - \vec{t}/3$  corresponds to "monoclinic kaolinite" having an unfavorable arrangement of cations in adjacent layers.

Tchoubar *et al.* (1982) employed another set of variables using the vacancy displacement model. Their version implied a preference for B layers alternating at random with A and C layers. Thus, thick blocks of "wrong" layers are not formed. The amount of different types of interlayers, however, increases, layer sequences B-C-B and B-A-B being the most frequent. The first sequence seems to be the same sequence as in dickite, and the presence of this sequence has been equated with the appearance of dickite nuclei within a kaolinite crystal (Plançon and Tchoubar, 1977c; Brindley *et al.*, 1986). In fact, it is only the B-C sequence that approximates that in dickite. The stacking in the fragments C-B and A-B correspond to that in "monoclinic kaolinite."

The reliability of X-ray diffraction profile analysis for the study of defect structures requires special attention. Plançon and Tchoubar (1977) showed that the diffraction theory for defect layer structures is sufficiently developed to allow a quantitative comparison of experimental and calculated diffraction profiles. If the experimental and calculated profiles do not match in their major details, the proposed model clearly does not adequately describe the real structure. A close match between the two, however, is insufficient to prove the correctness of the model. It is surprising that diffraction patterns from kaolinites of similar types can be described using the same model, but with very different sets of parameters. The only possible explanation is that the vacancy displacement model contains far too many variables. Thus, profile analysis for selected fragments of the diffraction pattern is not always sufficiently reliable for multiparametric models.

In addition to crystal chemical considerations, some experimental data suggest the absence of different types of layers in kaolinite, at least in large proportions. Using electron microscopic decoration techniques, Samotoin (1966) found that the growth steps in kaolin-group minerals formed different patterns. In kaolinite the growth steps show continuous terraces, whereas in dickite the pattern is that of intersecting steps, due to changing growth rates for adjacent layers in a given direction. Such intersections were never observed for kaolinite, which implies that all the layers are identical.

## ALTERNATIVE STACKING FAULT MODELS

### *Defects in crystals characterized by one layer type*

The symmetrical arrangement of atoms with respect to the *n* plane in kaolinite layers suggests a simple model for stacking faults. Assume that the displacement of a layer with respect to the previous one is described by the translation  $\vec{t}_1$ . If a regular crystal is formed, all successive layers are shifted by the same vector  $\vec{t}_1$ . A stacking fault may appear if a layer is formed that is related to the previous one by the plane *n*. In other words, *n* acts as a glide plane just for these two layers. Both the periodicity and the cation distribution pattern in the "defect" layer would remain unaffected. Therefore, the formation of such a layer would lead only to minor changes in the potential energy (as represented, e.g., by the electrostatic energy) of layer interaction, as well as in the hydrogen bond energy. Logically  $\vec{t}_2$ , which is related to  $\vec{t}_1$  by the same glide plane *n*, would be the new translation for a fragment between the "defect" layer in question and the next stacking fault. The second defectless fragment thus formed would be enantiomorphic to the first one. Thus, in terms of this model, stacking faults result from micro-intergrowth of right- and left-hand kaolinite crystals. If, by analogy to dickite, the pseudosymmetry of the kaolinite layer is close to the true symmetry, a layer reflected by the *n* plane would coincide with itself, because in kaolinite planes *n* and *m* coincide (Figures 2 and 3). Thus, the model of alternating enantiomorphic layers becomes that of alternating identical layers stacked with symmetrical translations  $\vec{t}_1$  and  $\vec{t}_2$ .

In terms of the conventional coordinate system  $\{a_1b_1\gamma_1\}$ , the projection of  $\vec{t}_1$  on the *ab* plane is  $(-0.369, -0.024)$ . The corresponding coordinates for  $\vec{t}_2$  are readily calculated from  $\vec{t}_1 = 1.901 \text{ \AA}$  and the angle  $\delta = 7^\circ$  between  $\vec{t}_1$  and  $-\vec{a}_1$ . Vectors  $\vec{t}_1$  and  $\vec{t}_2$  differ by the vector  $\vec{\tau} = (0.017, 0.328)$ . It can be easily shown that  $\vec{\tau} = (0, b/3)$ , if  $b/a = \sqrt{3}$  and  $\vec{t}_1 = -\vec{a}/3$ . The present model is a version of that proposed by Brindley and Robinson (1946), but it has been extended to account for the real crystal structure. The model proposed here not only differs from the model having  $\pm b/3$  shifts by a more realistic value for  $\vec{\tau}$ , but also it excludes the unfavorable stacking resulting from  $\vec{t}_1 - \vec{\tau}$  translations.



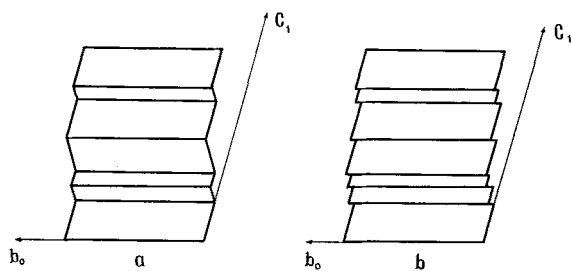


Figure 5. Kaolinite defect crystal for low contents of defects. (a) growth faults; (b) mechanical displacements.

The model is in agreement with the pattern of the growth pyramids observed in kaolinites, as displacements of identical layers have no effect on the growth rate in any direction. The  $\pm b/3$  defects are usually attributed to mechanical treatment after, e.g., resedimentation. The model in question can describe mechanical defects as well as crystal growth defects depending on the assignment of the appropriate parameters. For short-range ordering,  $S = 1$ , the parameters involved are the proportions  $W_i$  for the translation  $\vec{t}_i$  and one of the probabilities  $p_{ij}$  ( $i, j = 1, 2$ ) for  $\vec{t}_j$  to succeed  $\vec{t}_i$ .

#### Crystal growth stacking faults

The equivalence of the left- and right-handed unit cells for a regular kaolinite suggests equal proportions of both translations in a general assemblage of crystallites:  $W_1 = W_2 = 0.5$ . All  $p_{ij}$  values can therefore be calculated if one of them, e.g.,  $p_{11}$ , is specified. Obviously, this parameter may vary from 0 to 0.5, i.e., from perfectly ordered to a random alternation of  $\vec{t}_1$  and  $\vec{t}_2$ , and from 0.5 to 1 in the region of segregation. A crystal having growth defects for  $p_{11} > 0.5$  is shown schematically in Figure 5a. Figure 6 presents typical fragments of X-ray powder diffraction patterns in the 02,11 region. For  $p_{11} = 1$  the diffraction pattern is that of a sample consisting of equal proportions of regular right-handed and left-handed crystals. For  $p_{11} = 0.9$ , the sample is largely a mixture of regular and twinned crystals. Continued decrease in  $p_{11}$  to 0.5 leads to a smoothing of the modulations and a redistribution of the intensities. Although maximum maximum disorder corresponds to  $p_{11} = 0.5$  in the given angle range, reflections are smeared most for  $p_{11} = 0.65$ .

For  $0 \leq p_{11} < 0.5$ , modulations appear that have d-values unusual for kaolinite. In the limiting case of  $p_{11} = 0$ , the powder pattern corresponds to a two-layer kaolin-group polytype. Its nature is discussed below. X-ray powder diffraction patterns in the 20,13 reflection region change little for  $p_{11}$  values of 0 to 1.

The above set of parameters describes the model based on a symmetrical 1:1 layer. In defect crystals, layers may be distorted, such that the  $\{a_1, b_1, \gamma_1\}$  and  $\{a_2, b_2, \gamma_2\}$  cells are not exactly equivalent. Here, the pro-

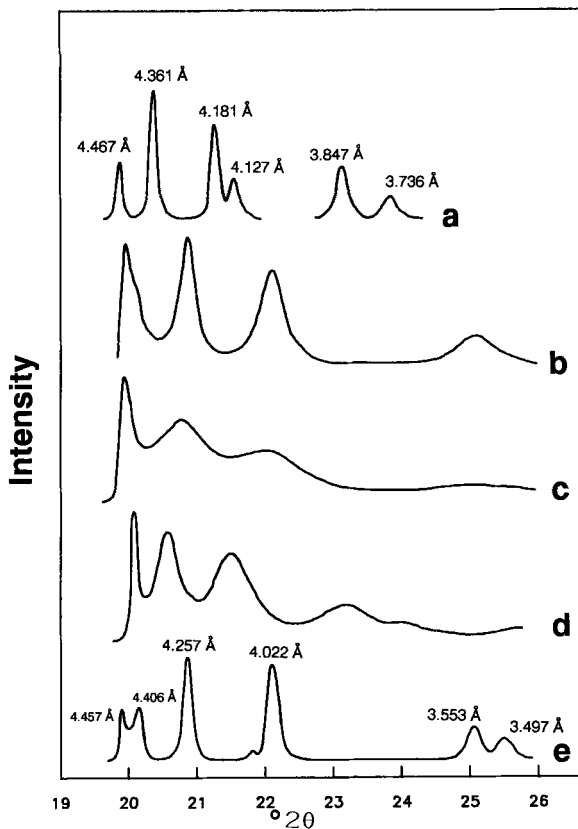


Figure 6. Simulated X-ray powder diffraction profiles for the one-layer model in the 02,11 reflections region (growth faults) (a)  $p_{11} = 1$ ; (b)  $b_{11} = 0.75$ ; (c)  $p_{11} = 0.5$ ; (d)  $p_{11} = 0.25$ ; (e)  $p_{11} = 0$ .

portion of one of the translations may be greater than the other, and an additional parameter,  $W_1$ , ranging from 0 to 1 is required, which, however, does not affect the essence of the model.

#### Stacking faults from post-crystallization mechanical effects

A comparison of Figures 5a and 5b illustrates the difference between growth and mechanical defects. A defect crystal shown in Figure 5b was obtained from an initially regular crystal,  $\vec{t}_1$  having undergone block displacements  $\vec{r}$  resulting from mechanical action. Here, only thin blocks of initial kaolinite were found, whereas enantiomorphic blocks were not found. For a random distribution of  $\vec{t}_1$  and  $\vec{t}_2$ , the content of faults,  $W_2$ , is the only independent variable. Figure 7 shows X-ray powder diffraction patterns for the 02,11 reflection region for a completely disoriented sample having different  $W_2$  values. Qualitatively, these diffraction patterns are similar to those for crystal growth defects, although, for low  $W_2$ , there is a quantitative difference. Therefore, in deciding whether an experimental distinction between these two fundamentally different

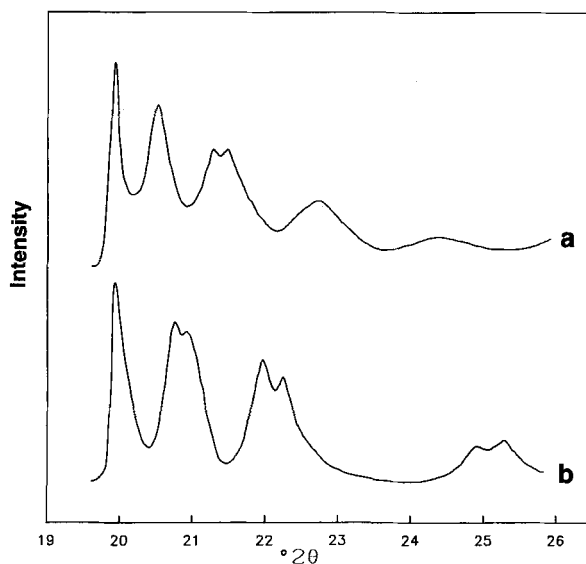


Figure 7. Simulated X-ray powder diffraction profiles for mechanical shifts model in the 02,11 reflections region. (a)  $W_2 = 0.2$ ; (b)  $W_2 = 0.4$ .

sources of faults can be made for a crystal containing both mechanical and growth defects is a problem.

#### Stacking faults in crystals with two types of layers

A comparison of the kaolinite and dickite unit cells has shown that a deviation of  $\gamma_1$  from  $90^\circ$  leads to an inequivalence of the B and C sites (*vide supra*). Therefore, the vacancy in regular kaolinite is always near the acute  $\gamma_1$  angle (Figure 3). Due to the minor difference between  $\gamma_1$  and  $90^\circ$ , however, a vacancy, as if by mistake, may occupy the C site. As shown above, the interlayer shift is defined unambiguously by the vacant site in the preceding layer (for a given choice of  $z$ -direction from tetrahedra to octahedra). Hence, the translation for the sequence B-C is  $\vec{t}_1$ . Inasmuch as kaolinite samples consisting of C layers have not been found in nature, defect fragments consisting of a considerable number of C layers should be absent. Therefore, a B layer should form soon after a C layer. The translation for the sequence C-B has the opposite sign before the  $y$ -component:  $\vec{t}_1' = (-0.369, 0.024)$ .

The content of C layers and  $p_{ij}$  values are the necessary variables here. A random distribution of C layers is the simplest case. For few C layers, B-C-B will be the most probable sequence. The use of  $S = 2$  allows the description of longer fragments of the type [-B-C-]. According to the vacancy position and the type of interlayer displacements, such defect fragments are, to a first approximation, similar to fragments of the dickite structure. Differences are due to the wrong  $\beta$  and  $\gamma$  angles, as compared with the dickite unit cell.

For  $W_2 \leq 0.1$ , changes in the X-ray powder patterns

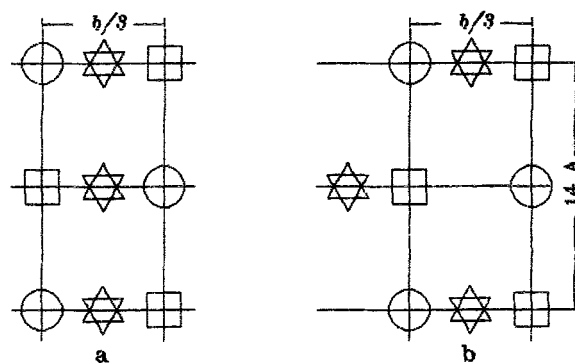


Figure 8. Arrangement of vacant and occupied octahedra and the centers of the hexagonal rings in consequent layers of dickite (a) and halloysite (b). Circles = occupied sites; squares = vacant sites; hexagons = centers of the hexagonal rings.

for the  $02l,11l$  reflections are similar to those described for the previous model. A fundamentally new difference arises for the 20,13 regions and consists in a shift of the  $hkl$  and  $h\bar{k}l$  reflections closer together. Such diffraction patterns have been observed for natural kaolinite samples and were attributed to  $\alpha$  drawing closer to  $90^\circ$ . Plançon and Tchoubar (1977b) introduced a special parameter  $C_M$  modifying angles  $\alpha$  and  $\beta$ . In terms of the present model, the distances between the reflections mentioned decrease automatically.

The idea that a vacancy may occupy a wrong site is a common feature of the present model and of the model proposed by Plançon and Tchoubar (1977b). The set of translations used changes both the crystal chemical nature of the stacking faults and the diffraction consequences of their presence in a crystal.

#### SUMMARY AND CONCLUSIONS

The study of defects in layer minerals by the analysis of the X-ray powder diffraction profiles is complicated by a number of factors. On one hand, different defects may lead to similar diffraction effects due, e.g., to the symmetry of the tetrahedral and octahedral sheets. On the other hand, difficulties arise because of the many variables that are generally used to describe the models. Therefore, models having very different physical characteristics may lead to an apparently satisfactory agreement between the simulated and experimental profiles.

In the present paper stacking faults have been assumed to be a natural consequence of the peculiarities of the real structure of the mineral. This approach excludes a number of previous models, while others are simplified, reducing the number of variables.

Two models are herein proposed involving one- and two-layer types. Qualitatively, X-ray powder diffraction patterns from kaolinites having few defects can be equally well described in terms of either model. In-

creasing the number of defects and especially the variations in their distribution, however, lead to dramatically different diffraction patterns for the two models.

It should be stressed that both models can describe the transformation of regular kaolinite via disordered phase into a regular two-layer kaolin-group polytype. In terms of the two-layer type model, this polytype is, apparently, dickite. The possibility of a continuous transition from regular kaolinite via disordered kaolinite and then from disordered dickite to regular dickite was discussed by Brindley *et al.* (1986). In terms of the one-layer type model, a regular alternation of two types of translations leads to a structure similar to that described by Chukhrov *et al.* (1966) for halloysite. Thus, another series of defect kaolinites may occur in nature, the end member being the structural analog of halloysite. Figure 8 shows the arrangement of vacant and filled octahedral sites and the centers of the hexagonal rings in the alternating layers for structures having one- and two-layer types. Vacant octahedra are identically arranged in both structures; however, although in dickite the centers of the hexagonal rings remain in the same *ac* plane, in halloysite they are alternately shifted by *b/3*.

Comparison of experimental and simulated X-ray powder diffraction patterns for the models described should elucidate the nature of defects in kaolinites and determine whether both defect-kaolinite series exist.

#### ACKNOWLEDGMENTS

We are indebted to R. F. Giese for improving the English of the manuscript.

#### REFERENCES

- Adams, J. M. and Hewat, A. W. (1981) Hydrogen atom positions in dickite: *Clays & Clay Minerals* **29**, 316–319.
- Bailey, S. W. (1980) Structures of layer silicates: in *Crystal Structures of Clay Minerals and their X-ray Identification*, G. W. Brindley and G. Brown, eds., Mineralogical Society, London, 495 pp.
- Blount, A. M., Threadgold, I. M., and Bailey, S. W. (1969) Refinement of the crystal structure of nacrite: *Clays & Clay Minerals* **17**, 185–194.
- Brindley, G. W. (1961) Kaolin, serpentine, and kindred minerals: *The X-ray Identification and Crystal Structures of Clay Minerals*, G. Brown, ed., Mineralogical Society, London, 51–131.
- Brindley, G. W. (1980) Order-disorder in clay minerals: in *Crystal Structures of Clay Minerals and their X-ray Identification*, G. W. Brindley and G. Brown, eds., Mineralogical Society, London, 495 pp.
- Brindley, G. W. and Robinson, K. (1946) Randomness in the structures of kaolinitic clay minerals: *Trans. Faraday Soc.* **42B**, 198–205.
- Brindley, G. W., Kao, C., Harrison, J. L., Lipsicas, M., and Raythatha, R. (1986) The relation between structural disorder and other characteristics of kaolinite and dickite: *Clays & Clay Minerals* **34**, 239–249.
- Chukhrov, F. V., Zvyagin, B. B., Rudnitskaya, E. S., and Ermilova, L. P. (1966) The nature and genesis of halloysite: *Izv. Akad. Nauk S.S.S.R., Ser. Geol.* **1966**, 3–20.
- Drits, V. A. and Kashaev, A. A. (1960) An X-ray diffraction study of a single crystal of kaolinite: *Soviet Phys. Crystallogr.* **5**, 207–210.
- Giese, R. F. (1982) Theoretical studies of the kaolin minerals: Electrostatic calculations: *Bull. Mineral.* **105**, 417–424.
- Goodyear, B. and Duffin, M. A. (1961) An X-ray examination of an exceptionally well crystallized kaolinite: *Mineral. Mag.* **32**, 902–907.
- Joswig, W. and Drits, V. A. (1986) The orientation of the hydroxyl groups in dickite by X-ray diffraction: *N. Jb. Miner. Mh.* **H1**, 19–22.
- Mitra, G. B. and Bhattacharjee, S. (1970) X-ray diffraction studies of the transformation of kaolinite into metakaolin: Study of layer shift: *Acta Crystallogr.* **B26**, 2124–2128.
- Murray, H. H. (1954) Structural variations of some kaolinites in relation to dehydrated halloysite: *Amer. Mineral.* **39**, 97–108.
- Newnham, R. E. (1961) A refinement of the dickite structure and some remarks on polymorphism in kaolin minerals: *Mineral. Mag.* **32**, 683–704.
- Noble, F. R. (1971) A study of disorder in kaolinite: *Clay Miner.* **9**, 71–81.
- Plançon, A. (1981) Diffraction by layer structures containing different kinds of layers and stacking faults: *J. Appl. Crystallogr.* **14**, 300–304.
- Plançon, A. and Tchoubar, C. (1977a) Determination of structural defects in phyllosilicates by X-ray diffraction. I. Principle of calculation of the diffraction phenomenon: *Clays & Clay Minerals* **25**, 430–435.
- Plançon, A. and Tchoubar, C. (1977b) Determination of structural defects in phyllosilicates by X-ray diffraction. II. Nature and proportion of defects in natural kaolinites: *Clays & Clay Minerals* **25**, 436–450.
- Rozdestvenskaya, I. V., Bookin, A. S., Drits, V. A., and Finko, V. I. (1982) Proton positions and structural peculiarities of dickite by X-ray diffraction: *Mineral. Zh.* **4**, 52–58 (in Russian).
- Sakharov, B. A., Naumov, A. S., and Drits, V. A. (1982) X-ray diffraction by mixed-layer structures having abundant distribution of stacking faults: *Dokl. Akad. Nauk S.S.S.R.* **265**, 339–343.
- Samotoin, N. D. (1966) Study of surface of kaolinite and dickite monocrystals by decoration method: *Zap. Vses. Mineral. Obshch.* **95**, 390–399.
- Sen Gupta, P. K., Schlemper, E. O., Johns, W. D., and Ross, F. (1984) Hydrogen positions in dickite: *Clays & Clay Minerals* **32**, 483–485.
- Suitch, P. R. and Young, R. A. (1983) Atom position in highly ordered kaolinite: *Clays & Clay Minerals* **31**, 357–366.
- Tchoubar, C., Plançon, A., Ben Brahim, J., Clinard, C., and Sow, C. (1982) Caractéristiques structurales des kaolinites desordonnées: *Bull. Minéral.* **105**, 477–491.
- Thompson, J. G. and Cuff, C. (1985) Crystal structure of kaolinite: dimethylsulfoxide intercalate: *Clays & Clay Minerals* **33**, 490–500.
- Zvyagin, B. B. (1960) Electron diffraction determination of the structure of kaolinite: *Soviet Phys. Crystallogr.* **5**, 32–41. (in Russian).
- Zvyagin, B. B. (1964) *Electron Diffraction Analysis of Clay Mineral Structures*: Nauka, Moscow (translation, 1967, Plenum Press, New York, 364 pp.).

(Received 11 October 1987; accepted 27 September 1988; Ms. 1735)